

SARS-CoV-2 virion stabilization by Zn binding

S. Morante^{a)b)*}, G. La Penna^{c)}, G.C. Rossi^{a)b)d)}, F. Stellato^{a)b)}

^{a)} Dipartimento di Fisica, Università di Roma “*Tor Vergata*”, Via della Ricerca Scientifica - 00133 Roma, Italy

^{b)} INFN, Sezione di Roma 2, Via della Ricerca Scientifica - 00133 Roma, Italy

^{c)} CNR, Institute for Chemistry of Organometallic Compounds - 50019 Sesto Fiorentino, Italy.

^{d)} Centro Fermi - Museo Storico della Fisica e Centro Studi e Ricerche “Enrico Fermi”, Piazza del Viminale - 00184 Roma, Italy

Abstract

Zinc plays a crucial role in the process of virion maturation inside the host cell¹. The accessory Cys-rich proteins expressed in SARS-CoV-2 by genes ORF7a and ORF8 are likely involved in zinc binding and in interactions with cellular antigens activated by extensive disulfide bonds. In this report we provide a proof of concept for the feasibility of a structural study of orf7a and orf8 proteins. We make the point that lack of cellular zinc, or substitution thereof, might lead to a significant slowing down of viral maturation.

*Corresponding author email: silvia.morante@roma2.infn.it

1 Introduction

The SARS-CoV-2 open reading frames ORF7a and ORF8 code for virion non-structural, called accessory², proteins of unknown function (orf7a and orf8, respectively, hereafter). The protein orf7a is common to all SARS-CoV type coronaviruses and highly conserved³, while orf8 is remarkably different from proteins coded by genes ORF8 and ORF8b of human SARS-CoV⁴.

The orf7a protein of SARS-CoV-1 has been shown to interact with several host proteins⁵. A similar situation has been reported in the case of the very similar SARS-CoV-2 orf7a protein⁶. The most supported hypothesis proposed for orf7a protein function is the interference with virion budding tethering⁷ operated by cellular antigens⁸. Indeed, orf7a is expressed in the host cell to inhibit the intracellular (at endoplasmic membrane) process of virion immobilization before and after virion vesiculation. On the basis of structural similarities we argue that also protein orf8 can be involved in the same inhibition process, strengthening the inhibition of virion immobilization. This conjecture is in agreement with Ref. 6 where it is suggested that orf8 plays a role in vesicle trafficking and in endoplasmic reticulum protein quality control, thus favouring the reconfiguration of ER/Golgi trafficking during coronavirus infection.

Virion tethering is mainly due to proteins of the tetherin family, also known as bone marrow stromal antigen 2 (BST2) or cluster of differentiation 317 (CD317). BST2 is expressed in many cells in the interferon-dependent antiviral response pathway. The mechanism of tethering involves tetherin protein dimerization via formation of extended disulfide bonds within the coiled coil region⁹. This step is strongly influenced by divalent cations involved in Cys binding. Among these ions, the most available in cells is Zn²⁺.

A timely computational search for therapeutic targets of SARS-CoV-2 found the orf7a-BST2 complex as a potential target to be addressed with structural studies¹⁰.

The orf7a and orf8 protein sequences (both 121 amino acids long) hint at a high Zn binding propensity, as they display 6 Cys/3 His and 7 Cys/4 His sidechains, respectively, with motifs that are able to bind Zn, thus forming multiple zinc finger (ZF) domains. The relevance of Zn in the viral replication process has been widely investigated^{1,11} and, indeed, two ZF domains have been discovered in the nucleocapsid protein of HIV-1 (Ncp7)^{12,13}. Two such similar Zn domains have been also identified¹⁴ along the highly conserved, within the SARS-CoV family⁴, nsp12 polymerase.

2 Method and Results

The pivotal role of Zn in SARS-CoV replication has been demonstrated by inhibition of RNA polymerase activity both *in vitro* and in cell culture¹⁵.

Comparing with the well assessed ZF domains of Ncp7 CX₂CX₄HX₄C (located from aa 15 to aa 28 and from aa 36 to aa 49), one identifies the similar CX₃HX₃C and CX₈CX₅H motifs in orf7a (located from aa 15 to aa 23 and from aa 56 to aa 73, respectively) and the HX₂CX₄CX₂H motif in orf8 (located from aa 17 to aa 28). The patterns of these motifs are shown in Fig 1.

UNIPROT (https://www.uniprot.org/help/zn_fing) reports a large variety of ZF domains among which also the Cys-rich patterns of orf7a and orf8 can be accommodated.

From a structural point of view it is not difficult to come up with a plausible protein structure capable of hosting a Zn²⁺ ion. Focusing on orf7a as an example, one can proceed to construct such structures by first building an atomistic model of the protein in a random coil configuration. After simulating self-avoiding random walks^{16,17} of the chain in vacuum by randomly changing the dihedral angles (not involving H atoms) of all residues (except Φ in Pro), for a total of 445 dihedral angles, we proceeded by monitoring along the trajectory the distance d between pairs of S γ (Cys)-S γ (Cys) atoms, $d(\text{CC})$, and S γ (Cys)-N ϵ (His) atoms, $d(\text{CH})$. All His sidechains are neutral and protonated at N δ . We collected a trajectory of 400 random configurations, with consecutive configurations separated by 500 attempted torsional moves. Acceptance ratio was about 0.5. Two chain configurations where three among all of the possible $d(\text{CC})$ and $d(\text{CH})$ distances are smaller than 1.2 nm were selected. This condition was found to be satisfied by the triplets

Zinc Finger Domains

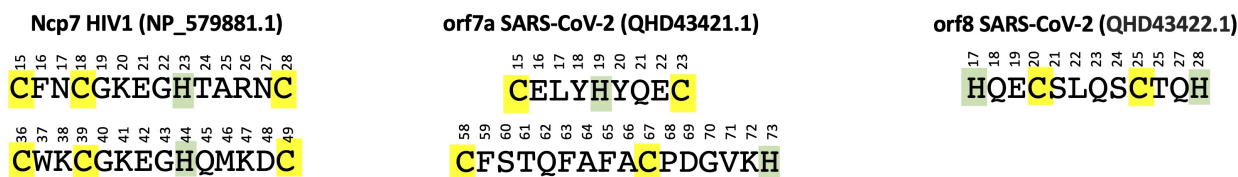


Figure 1: ZF domains in NP.579881 (Ncp7 of HIV-1) (left), QHD43421.1 (orf7a of SARS-CoV-2) (center) and QHD43422.1 (orf8 of SARS-CoV-2) (right). Cys are highlighted in yellow and His in green.

Cys(15)...His(19)...Cys(23) in one case and Cys(58)...Cys(67)...His(73) in a second case. Zn^{2+} ions were then inserted at the geometric center of each of the two selected triplets of atoms. A cationic dummy atom model for Zn^{18} and the PARM14 Amber force-field¹⁹ for the protein were used. We took a distance cut-off for non-bonding interactions of 0.5 nm, with Coulomb interactions shifted and damped to achieve local neutralization²⁰. These conditions mimic size distribution of small proteins when simulated in vacuum. Starting from the selected configurations, we relaxed the systems by classical molecular dynamics. At the beginning, harmonic forces with $k = 10 \text{ kcal/mol/\AA}^2$ were added to bring the distances between Zn and the three atoms [$S\gamma(\text{Cys}(15))$, $N\epsilon(\text{His}(19))$, $S\gamma(\text{Cys}(23))$] in the first case (site Zn-CHC) and [$S\gamma(\text{Cys}(58))$, $S\gamma(\text{Cys}(67))$, $N\epsilon(\text{His}(73))$] in the second (site Zn-CCH) from the initial values down to 2.5 Å in 10 ps. The energy of the system was then minimized. The final configurations of sites Zn-CHC (segment 15-23) and Zn-CCH (segment 58-73) are displayed in Figs. 2, left and right panels, respectively. All calculations were performed with the LAMMPS code²¹.

We interpret the fact that we have been able to easily get Zn-CHC and Zn-CCH stable configurations already with very simple simulation techniques, as a strong indication of the high propensity to form ZF domains as soon as the occurrence frequency of Cys and His along the protein sequence (or in its environment) is sufficiently high.

3 Discussion

Based on the above considerations, the main point we want to make in this report is that, although the affinity of ZF domains for Zn is larger than for other divalent cations of similar size available in cells, like Mg^{2+} , Zn^{2+} can be displaced upon altering concentration in host cells by temporary Zn deprivation and Mg augmentation. Thus, cellular Zn deprivation, Zn replacement by Mg and/or specific drugs based on Ag(I) and Au(I)²², might result in a significant slowing down of viral replication, owing to the inhibition of orf7a/BST2 and orf8/BST2 complexes formation. Circumstantial support for this hypothesis comes from the well-known, important role played by Zn in inflammation^{23,24}.

According to the scenario we have described, we are engaged in the project of producing atomistic models of the orf7a/BST2 and orf8/BST2 complexes, that can serve as reliable templates in the analysis of the forthcoming experiments aimed at unveiling the detailed structure of these systems.

The comparison to known related structures, *i.e.* the N-terminal ectodomain of orf7a of SARS-CoV-1 in the absence of Zn^{25} (PDB 1XAK) and Ncp7 of HIV-1 in the presence of Zn^{12} (PDB 1ESK), will be the basis to model BST2 disulfide bond plasticity induced by modulation of orf7a/orf8 Zn-binding.

The resulting structures will also be useful for further experimental studies aimed at validating (or disproving) the function of orf7a/orf8 proteins as diversion tools of the interferon-dependent antiviral response.

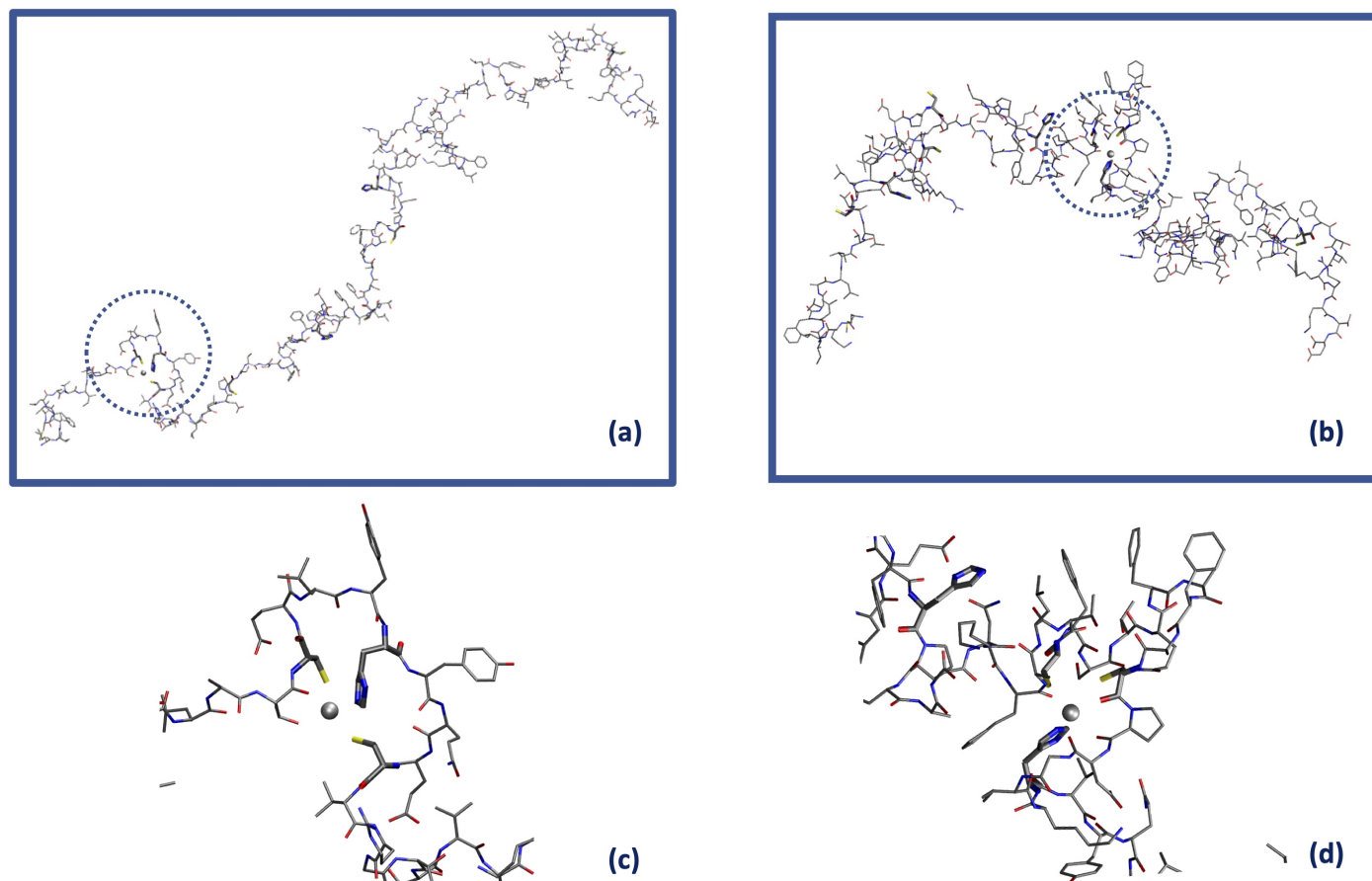


Figure 2: Sketch of orf7a structures capable of hosting a Zn^{2+} ion (gray sphere) within the **CELYHYQEC** 15-23 segment (Zn-CHC, left) and the **CFSTQFAFACPDGVKH** 58-73 segment (Zn-CCH, right). Cys and His residues are highlighted in bold. Panel (c) and (d) represent the blow-up of the local Zn^{2+} binding sites Cys(15)-His(19)-Cys(23) (circled in panel (a)) and Cys(58)-Cys(67)-His(73) (circled in panel (b)), respectively.

References

- [1] U. C. Chaturvedi and R. Shrivastava, *FEMS Immun. Med. Microbiol.*, 2005, **43**, 105–114.
- [2] *Retroviruses*, ed. J. M. Coffin, S. H. Hughes and V. H. E., Cold Spring Harbor (NY): Cold Spring Harbor Laboratory Press, 1997.
- [3] A. Wu, Y. Peng, B. Huang, X. Ding, X. Wang, P. Niu, J. Meng, Z. Zhu, Z. Zhang, J. Wang, J. Sheng, L. Quan, Z. Xia, W. Tan, G. Cheng and T. Jiang, *Cell Host Microbe*, 2020, **27**, 325–328.
- [4] J. Xu, S. Zhao, T. Teng, A. E. Abdalla, W. Zhu, L. Xie, Y. Wang and X. Guo, *Viruses*, 2020, **12**, 244.
- [5] N. Vasilenko, I. Moshynskyy and A. Zakhartchouk, *Virol. J.*, 2010, **7**, 31–36.
- [6] D. E. Gordon, G. M. Jang, M. Bouhaddou, J. Xu, K. Obernier, K. M. White, M. J. O’Meara, V. V. Rezelj, J. Z. Guo, D. L. Swaney *et al.*, *Nature*, 2020, 1–13.
- [7] J. S. Bonifacino and B. S. Glick, *Cell*, 2004, **116**, 153–166.
- [8] J. K. Taylor, C. M. Coleman, S. Postel, J. M. Sisk, J. G. Bernbaum, T. Venkataraman, E. J. Sundberg and M. B. Frieman, *J. Virol.*, 2015, **89**, 11820–11833.
- [9] A. Le Tortorec, S. Willey and S. J. D. Neil, *Viruses*, 2011, **3**, 520–540.

- [10] C. Wu, Y. Liu, Y. Yang, P. Zhang, W. Zhong, Y. Wang, Q. Wang, Y. Xu, M. Li, X. Li, M. Zheng, L. Chen and H. Li, *Acta Pharm. Sin. B*, 2020.
- [11] C. T. Chasapis, *J. Inorg. Biochem.*, 2018, **186**, 157–161.
- [12] N. Morellet, H. Déméné, V. Teilleux, T. Huynh-Dinh, H. de Rocquigny, M.-C. Fournié-Zaluski and B. P. Roques, *J. Mol. Biol.*, 1998, **283**, 419–434.
- [13] J. Guo, T. Wu, J. Anderson, B. F. Kane, D. G. Johnson, R. J. Gorelick, L. E. Henderson and J. G. Levin, *J. Virol.*, 2000, **74**, 8980–8988.
- [14] R. N. Kirchdoerfer and A. B. Ward, *Nature Commun.*, 2019, **10**, 2342.
- [15] A. J. W. te Velhuis, S. H. E. van den Worm, A. C. Sims, R. S. Baric, E. J. Snijder and M. J. van Hemert, *PLoS Pathog.*, 2010, **6**, e1001176.
- [16] G. La Penna, S. Morante, A. Perico and G. C. Rossi, *J. Chem. Phys.*, 2004, **121**, 10725–10741.
- [17] S. Furlan, G. La Penna and A. Perico, *Macromolecules*, 2008, **41**, 2938–2948.
- [18] Y.-P. Pang, *Proteins: Struct., Funct., Bioinf.*, 2001, **45**, 183–189.
- [19] J. A. Maier, C. Martinez, K. Kasavajhala, L. Wickstrom, K. E. Hauser and C. Simmerling, *J. Chem. Theory Comput.*, 2015, **11**, 3696–3713.
- [20] D. Wolf, P. Keblinski, S. R. Phillpot and J. Eggebrecht, *J. Chem. Phys.*, 1999, **110**, 8254–8282.
- [21] S. Plimpton, *J. Comput. Phys.*, 1995, **117**, 1–19.
- [22] K. Kluska, M. D. Peris-Díaz, D. Płonka, A. Moysa, M. Dadlez, A. Deniaud, W. Bal and A. Krzel, *Chem. Commun.*, 2020, **56**, 1329–1332.
- [23] T. Dudev and C. Lim, *J. Phys. Chem. B*, 2001, **105**, 4446–4452.
- [24] N. Z. Gammoh and L. Rink, *Nutrients*, 2017, **9**, 624–637.
- [25] C. A. Nelson, A. Pekosz, C. A. Lee, M. S. Diamond and D. H. Fremont, *Structure*, 2005, **13**, 75–85.